

Thermal Decomposition Kinetics of Azomethine Oligomer and Its Some Metal Complexes

Fatih Doğan,¹ İsmet Kaya,² Ali Bilici,³ Mehmet Saçak⁴

¹Faculty of Education, Secondary Science and Mathematics Education, Çanakkale Onsekiz Mart University, Çanakkale 17100, Turkey

²Department of Chemistry, Çanakkale Onsekiz Mart University, Çanakkale 17020, Turkey

³Control Laboratory of Agricultural and Forestry Ministry, Çanakkale 17100, Turkey

⁴Department of Chemistry, Faculty of Science, Ankara University, Tandoğan, Ankara, Turkey

Received 19 December 2008; accepted 24 February 2010

DOI 10.1002/app.32355

Published online 21 May 2010 in Wiley InterScience (www.interscience.wiley.com).

ABSTRACT: In our previous study, we presented the synthesis, characterization, and some physical properties of a new azomethine oligomer and its some metal complexes. This study focuses on the thermal decomposition kinetics of these reported materials. The studied compounds were 1,4-bis[(2-hydroxyphenyl)methylene]phenylenediamine, oligo-1,4-bis[(2-hydroxyphenyl)methylene]phenylenediamine, and oligo-1,4-bis[(2-hydroxyphenyl)methylene]phenylenediamine–metal complexes. Several kinetic methods based on a single heating rate such as Coats-Redfern, MacCallum-Tanner, van Krevelen, Horowitz-Metzger, Wanjun-Yuwen-Hen-Cunxin, and Madhusudan-Krishnan-Ninan were used to elucidate the kinetic

parameters of the decomposition processes. The parameters such as activation energy E , frequency factor A , reaction order n , entropy change ΔS^* , enthalpy change ΔH^* , and Gibbs free energy change ΔG^* were calculated by means of the above methods. The activation energy values obtained by each method were in good agreement with each other. An appropriate mechanism for the thermal decomposition process of each material was also determined by means of the thermogravimetric analysis. © 2010 Wiley Periodicals, Inc. *J Appl Polym Sci* 118: 547–556, 2010

Key words: oligomer–metal complex; kinetic analysis; activation energy

INTRODUCTION

The first example of metal-containing polymers was reported by Arimoto and Haven.¹ Since then, the metal-containing polymers have been extensively studied by many researchers because of potential applications such as adhesives, high-temperature lubricants, electrical insulators, and semiconductors.^{1–4} These complexes are generally insoluble in common solvents and have multiactive sites within the molecule. This presents new possibilities for controlling catalytic properties.⁵ They also have good thermal stabilities because of their rigid backbone. Many studies have been dedicated to the synthesis of metal complexes of poly-Schiff bases. The thermal properties of Schiff base-substituted oligo/polyphenol and their metal complexes were investigated by Kaya and Bilici.^{6–8} Copper(II), zinc(II), and cobalt(II) complexes of oligosalicylaldehyde were synthesized, and their thermal properties were investigated by Mart and Vilayetoglu.⁹ The thermooxidative stability of chelate polymers based on

Schiff base was studied by Cazacu et al.¹⁰ Thermally stable Schiff-base polymers and their copper(II), cobalt(II), and nickel(II) complexes were reported by Tuncel et al.¹¹ Copper(II)-chelated polyazomethines were synthesized, and the influence of the copper content on the thermal behavior of this material was studied by Oriol et al.¹² In the decomposition kinetics study, the methods of Coats-Redfern (CR),¹³ Horowitz-Metzger (HM),¹⁴ Madhusudan-Krishnan-Ninan (MKN),¹⁵ van Krevelen (vK),¹⁶ Wanjun-Yuwen-Hen-Cunxin (WHYC),¹⁷ and MacCallum-Tanner (MC)¹⁸ were used for the calculation of kinetic parameters such as reaction order n , activation energy E , entropies ΔS^* , enthalpy change ΔH^* , free energy change ΔG^* , and preexponential factor A . The mechanism function related to each thermal decomposition process was also investigated by the Criado-Malek-Ortega method.¹⁹

In this study, the thermal decomposition kinetics of 1,4-bis[(2-hydroxyphenyl)methylene]phenylenediamine (HPMPDA), oligo-1,4-bis[(2-hydroxyphenyl)methylene]phenylenediamine (OHPMPDA), and some metal complexes of OHPMPDA are presented.

MATERIALS AND METHODS

Materials

Salicylaldehyde, *p*-phenylene diamine, methanol, ethanol, THF, KOH, hydrochloric acid (HCl, 37%),

Correspondence to: F. Doğan (fatihdogan@comu.edu.tr).

Contract grant sponsor: Ankara University Scientific Research Projects Commission; contract grant number: 2007-07-05-117.

Co(AcO)₂·4H₂O, Ni(AcO)₂·4H₂O, Cu(AcO)₂·H₂O, FeSO₄·7H₂O, Zn(AcO)₂·2H₂O, Pb(AcO)₂·3H₂O, MnCl₂·6H₂O, Cd(AcO)₂·2H₂O, and HgSO₄·H₂O were supplied by Merck Chemicals (Germany), and they were used as received. Sodium hypochlorite (NaOCl) (30% aqueous solution) was supplied by Paksoy Chemical (Turkey).

Oligomerization: General procedure

All compounds were prepared according to previous reported procedure.²⁰ The procedure is as follows:

Synthesis of oligomer

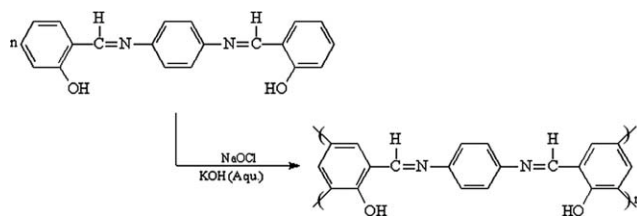
OHPMPDA was synthesized through oxidative polycondensation of HPMPDA with NaOCl solution (30%, in water) (Scheme 1). HPMPDA (0.316 g, 0.001 mol) was dissolved in an aqueous KOH solution (10%, 0.001 mol) and placed into a 50-mL three-necked round-bottom flask. The flask was fitted with a condenser, thermometer, stirrer, and an addition funnel containing NaOCl solution. After heating to 40°C, NaOCl solution was added drop by drop over about 20 min. The mixture was neutralized with 0.001 mol HCl (37%) at room temperature. Unreacted monomer was separated from the reaction products by washing with methanol. For the separation of mineral salts, the mixture was filtered and washed with 25 mL of hot water three times and then dried in an oven at 105°C.

Synthesis of oligomer–metal complexes

The solutions of Co(AcO)₂·4H₂O, Ni(AcO)₂·4H₂O, Cu(AcO)₂·H₂O, FeSO₄·7H₂O, Zn(AcO)₂·2H₂O, Pb(AcO)₂·3H₂O, MnCl₂·6H₂O, Cd(AcO)₂·2H₂O, and HgSO₄·H₂O (2 mmol) in methanol (10 mL) were added to a solution of oligomer (2 mmol/U) in THF (20 mL). The mixture was stirred for 3 h at room temperature. The precipitated complex was filtered, washed with cold methanol/THF (1 : 1), and then dried in a vacuum oven.

Thermal analysis

The thermal analyses were performed using a Perkin Elmer Diamond TG-DTA instrument. The measurements were recorded in a dynamic nitrogen atmosphere at a flow rate of 60 mL min⁻¹ and heated up to 1000°C. The heating rate was 10°C min⁻¹, and the mass of samples put into a platinum crucible was about 5 mg. α-Al₂O₃ was used as a reference material. All the experiments were performed two times for repeatability, and the results showed good repeatability with small variations in kinetic parameters.



Scheme 1 Synthesis of oligo-1,4-bis[(2-hydroxyphenyl)methylene] phenylene diamine

Kinetic parameters

The six methods investigated in this article were MKN, MC, WHYC, vK, CR, and HM as below.

Madhusudanan-Krishnan-Ninan method

$$\ln \left[\frac{g(\alpha)}{T^{1.9206}} \right] = \ln \left(\frac{AE}{\beta R} \right) + 3.7678 - 1.9206 \ln E - 0.12040 \left(\frac{E}{T} \right). \quad (1)$$

MacCallum-Tanner method

$$\log g(\alpha) = \log \left(\frac{AE}{\beta R} \right) - 0.4828E^{0.4351} - \left(\frac{0.449 + 0.217E}{10^{-3}T} \right). \quad (2)$$

Wanjun-Yuwen-Hen-Cunxin method

$$\ln \left[\frac{g(\alpha)}{T^{1.8946}} \right] = \left[\ln \frac{AR}{\beta E} + 3.6350 - 1.8946 \ln E \right] - 1.0014 \left(\frac{E}{RT} \right). \quad (3)$$

van Krevelen method

$$\ln g(\alpha) = \ln \left[\frac{A(0.368/T_m)^{\frac{E}{RT_m}}}{\beta \left(\frac{E}{RT_m} + 1 \right)} \right] + \left(\frac{E}{RT_m} + 1 \right) \ln T. \quad (4)$$

Coats-Redfern method

$$\ln \left[\frac{g(\alpha)}{T^2} \right] = \ln \left[\frac{AR}{\beta E} \left(1 - \frac{2RT}{E} \right) \right] - \left(\frac{E}{RT} \right). \quad (5)$$

Horowitz-Metzger method

The Horowitz-Metzger method introduced a characteristic temperature T_m and a parameter θ as follows:

$$\theta = T - T_m.$$

If the reaction order is 1, T_m is defined as the temperature at which $(1 - \alpha)_m = 1/e = 0.368$ and the final expression becomes:

$$\ln \ln g(\alpha) = \frac{E\theta}{RT_m^2}.$$

If the reaction order is unknown, T_m is defined for the maximum heating rate.

TABLE I
Algebraic Expressions for the Most Frequently used Mechanisms of Solid State Processes

No	Mechanisms	Symbol	Differential form, $f(\alpha)$	Integral form, $g(\alpha)$
Sigmoidal curves				
1	N and G ($n = 1$)	A ₁	$(1 - \alpha)$	$[-\ln(1 - \alpha)]$
2	N and G ($n = 1.5$)	A _{1.5}	$(3/2)(1 - \alpha)[- \ln(1 - \alpha)]^{1/3}$	$[-\ln(1 - \alpha)]^{2/3}$
3	N and G ($n = 2$)	A ₂	$2(1 - \alpha)[- \ln(1 - \alpha)]^{1/2}$	$[-\ln(1 - \alpha)]^{1/2}$
4	N and G ($n = 3$)	A ₃	$3(1 - \alpha)[- \ln(1 - \alpha)]^{2/3}$	$[-\ln(1 - \alpha)]^{1/3}$
5	N and G ($n = 4$)	A ₄	$4(1 - \alpha)[- \ln(1 - \alpha)]^{3/4}$	$[-\ln(1 - \alpha)]^{1/4}$
Deceleration curves				
6	Diffusion, 1D	D ₁	$1/(2\alpha)$	α^2
7	Diffusion, 2D	D ₂	$1/(\ln(1 - \alpha))$	$(1 - \alpha)\ln(1 - \alpha) + \alpha$
8	Diffusion, 3D	D ₃	$1.5/[(1 - \alpha)^{-1/3} - 1]$	$(1 - 2\alpha/3) - (1 - \alpha)^{2/3}$
9	Diffusion, 3D	D ₄	$[1.5(1 - \alpha)^{2/3}][1 - (1 - \alpha)^{1/3}]^{-1}$	$[1 - (1 - \alpha)^{1/3}]^2$
10	Diffusion, 3D	D ₅	$(3/2)(1 + \alpha)^{2/3}[(1 + \alpha)^{1/3} - 1]^{-1}$	$[(1 + \alpha)^{1/3} - 1]^2$
11	Diffusion, 3D	D ₆	$(3/2)(1 - \alpha)^{4/3}[[1/(1 - \alpha)^{1/3}] - 1]^{-1}$	$[[1/(1 - \alpha)^{1/3}] - 1]^2$
12	Contracted geometry shape (cylindrical symmetry)	R ₂	$(1 - \alpha)^{1/2}$	$2[1 - (1 - \alpha)^{1/2}]$
13	Contracted geometry shape (sphere symmetry)	R ₃	$(1 - \alpha)^{1/3}$	$3[1 - (1 - \alpha)^{1/3}]$
Acceleration curves				
14		P ₁	1	α
15		P ₂	$2\alpha^{1/2}$	$\alpha^{1/2}$
16		P ₃	$(1.5)\alpha^{2/3}$	$\alpha^{1/3}$
17		P ₄	$4\alpha^{3/4}$	$\alpha^{1/4}$
18		P _{3/2}	$2/3(\alpha)^{-1/2}$	$\alpha^{3/2}$
19		P _{2/3}	$3/2(\alpha)^{1/3}$	$\alpha^{2/3}$
29		P _{3/4}	$4/3(\alpha)^{-1/3}$	$\alpha^{3/4}$

When $\theta = 0$, $(1 - \alpha) = (1 - \alpha)_m$ and $(1 - \alpha)_m = n^{1/1-n}$ and

$$\ln \left[\frac{1 - (1 - \alpha)^{1-n}}{(1 - n)} \right] = \ln \frac{ART_m^2}{\beta E} - \frac{E}{RT_m} + \frac{E\theta}{RT_m^2}. \quad (6)$$

In the equations above, α , $g(\alpha)$, β , T_m , E , A , and R are the degree of reaction, integral function of conversion, heating rate, DTG peak temperature, activation energy (kJ mol⁻¹), preexponential factor (min⁻¹), and gas constant (8.314 J mol⁻¹ K⁻¹), respectively.

Criado-Malek-Ortega method

If the value of the activation energy is known, the kinetic model of the process can be determined by this method. Criado et al. define the function:

$$z(\alpha) = \frac{\left(\frac{d\alpha}{dt}\right)}{\beta} \pi(x)T, \quad (7)$$

where $x = E/RT$, and $\pi(x)$ is an approximation of the temperature integral, which cannot be expressed in a simple analytical form. In this case, the fourth rational expression of Senum and Yang²¹ is used. Combining a rate expression, $\frac{d\alpha}{dt} = kf(\alpha)$ and eq. (7), we can obtain:

$$z(\alpha) = f(\alpha)F(\alpha). \quad (8)$$

Then, the master curves of different models listed in Table I can be obtained following this function. The mechanism of a solid-state process can be determined by comparing the $z(\alpha)$ plots calculated by eq. (7) using experimental data with the master curves.

The activation entropy ΔS^\ddagger , the activation enthalpy ΔH^\ddagger , and the free activation energy of activation ΔG^\ddagger were calculated using the following equations²²:

$$\Delta S^\ddagger = 2.303 \left(\log \frac{Ah}{kT_m} \right) R \quad (9)$$

$$\Delta H^\ddagger = E - RT_m \quad (10)$$

$$\Delta G^\ddagger = \Delta H^\ddagger - T_m \Delta S^\ddagger, \quad (11)$$

where $f(\alpha)$, k , and h are so-called kinetic function that depends on the reaction mechanism, Boltzmann constant, and Planck constant, respectively.

In this study, kinetic methods based on a single heating rate were used. The linearization curves of each decomposition step for the studied systems

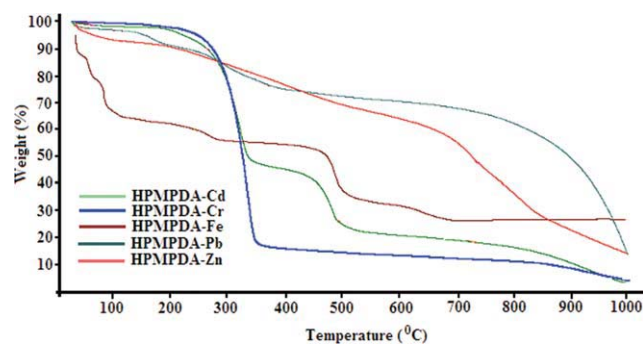


Figure 1 TG curves of OHPMPDA-Cd, OHPMPDA-Cr, OHPMPDA-Fe, OHPMPDA-Pb, and OHPMPDA-Zn metal complexes. [Color figure can be viewed in the online issue, which is available at www.interscience.wiley.com.]

were determined using the least squares method. The kinetic and thermodynamic parameters were calculated by the software developed in our laboratory using PHP Web programming language.²³

RESULTS AND DISCUSSION

Thermal stability

The thermodynamic and thermal properties of HPMPDA, OHPMPDA, and OHPMPDA-metal complexes [M = Cr(III), Mn(II), Fe(II), Co(II), Ni(II), Cu(II), Zn(II), Cd(II), Hg(II), and Pb(II)] were studied by thermogravimetric analysis (TGA) from ambient temperature to 1000°C under nitrogen atmosphere. TG/DTG curves and DTA profiles of HPMPDA, OHPMPDA, and OHPMPDA-metal complexes were presented in our previous study.²⁰ These profiles are also given in Figures 1 and 2. The initial and final temperatures, and decomposition functions in addition to total mass losses of each step in the thermal decomposition of all compounds are given in Table II. As seen from Figures 1 and 2, most of the curves exhibit similar characteristics.

HPMPDA shows one decomposition stage in the temperature range of 208–527°C with a 85.71% weight loss. The DTA profile exhibited two endothermic thermal effects at 183 and 371°C. First peak corresponds to the melting point of HPMPDA, whereas the last, at 371°C, peak corresponds to the decomposition of HPMPDA. It appears from the TG curve that OHPMPDA is decomposed in one stage over the temperature range of 233–360°C. As seen from the DTA profile, two endothermic peaks for OHPMPDA are noted. These peaks are found at 201 and 284°C. Although the first (201°C) was attributed to the melting of OHPMPDA, the second (284°C) was assigned to the decomposition of OHPMPDA. The thermal decomposition processes of OHPMPDA-Zn involve two stages. These stages are between 158 and 604°C and 604 and 997°C, respec-

tively, with mass losses of 37.7 and 49.7%. The DTA profile of this complex presents two endothermic effects at 378 and 710°C. OHPMPDA-Pb, OHPMPDA-Cd, and OHPMPDA-Cu thermally decomposed in two successive decomposition steps. The first decomposition step of OHPMPDA-Cu estimated a mass loss of 10% within the temperature range from 100 to 226°C. The last step was between 226 and 608°C. The decomposition stages for OHPMPDA-Cd occur between 176 and 407°C and 407 and 648°C, with mass losses of 53.15 and 36.55%, respectively. The DTA profile shows three endothermic peaks at 212, 334, and 489°C. The first peak at 212°C corresponds to the melting of OHPMPDA-Cd.

The first estimated mass loss of 5.3% within the temperature range 40–106°C is assigned to the elimination of H₂O from the complex. OHPMPDA-Ni exhibits three successive decomposition stages in the temperature ranges of 42–136°C, 136–408°C, and 408–544°C with mass losses of 4.21, 22.33, and 39.89%, respectively. The carbon residue at 1000°C was found to be 33.57%.

The mass loss of 4.21% observed at the first stage is due to the elimination of H₂O. According to the TG/DTG curves of OHPMPDA-Mn, OHPMPDA-Mn exhibited four decomposition stages. OHPMPDA-Mn is thermally stable up to 41°C. The mass loss in the temperature ranges of 30–150°C corresponds to the dehydration of crystallization water from the complex. Three endothermic peaks at 206, 298, and 669°C were observed in the DTA profile. The first peak at 206°C is due to the melting of the complex.

The TG curve of OHPMPDA-Fe indicates mainly four main decomposition stages. These are in the temperature ranges of 76–135°C, 135–362°C, 422–600°C, and 600–722°C. Although the first two peaks of decomposition steps in temperature ranges of 46–76°C and 76–135°C correspond to the dehydration of crystallization water from the complex, the other peaks correspond to the decomposition of the

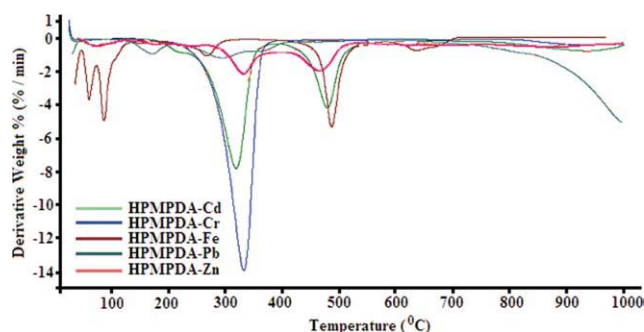


Figure 2 DTG curves of OHPMPDA-Cd, OHPMPDA-Cr, OHPMPDA-Fe, OHPMPDA-Pb, and OHPMPDA-Zn metal complexes. [Color figure can be viewed in the online issue, which is available at www.interscience.wiley.com.]

TABLE II
TG Data of Thermal Decomposition of HPMPDA, OHPMPDA and OHPMPDA-metal Complexes

Compound	Step	DTA peak (°C)	DTG _{max} (°C)	Temperature range (°C)	DTA	% Mass loss
OHPMPDA	I	201,284	273	233–360	endo, endo	56.25
	Residue			>360		43.75
HPMPDA	I	183, 371	365	208–527	endo, endo	85.71
	Residue			>527		14.29
OHPMPDA-Zn	I	378	381	158–604	endo	36.26
	II	710	746	604–997	endo	49.96
OHPMPDA-Pb	Residue			>997		13.78
	I		175	100–226		9.39
OHPMPDA-Ni	II		302	226–608		77.46
	Residue			>608		13.15
OHPMPDA-Ni	I		77	42–136		4.21
	II		336	136–408		22.33
	III		471	408–544		39.89
OHPMPDA-Mn	Residue			>544		33.57
	I		45	41–156	endo	4.51
OHPMPDA-Mn	II	206, 298	293	156–400	endo	17.93
	III	669	643	400–692	endo	27.25
	IV		758	692–807	endo	18.31
OHPMPDA-Mn	Residue			>807		32.10
	I		149	95–220		35.87
OHPMPDA-Hg	II		264	220–283		12.69
	III		335	283–450		24.46
	Residue		804	450–943		22.2
OHPMPDA-Fe				>943		4.78
	I	63	62	46–76	endo	21.81
	II	92	89	76–135	endo	8.79
	III	284	268	135–362	endo	11.99
	III	497	489	422–600	endo	31.39
OHPMPDA-Fe	IV	652	649	600–722	endo	5.22
	Residue			>722	endo	20.8
OHPMPDA-Cu	I		60	40–106		5.30
	II	314	316	183–758	exo	42.03
OHPMPDA-Cr	Residue			>758		52.67
	I	210, 346	336	221–407	endo, endo	83.97
OHPMPDA-Cr	Residue			>407		16.03
	I	529	536	222–731	endo	55.59
OHPMPDA-Co				>407		45.41
	I	212, 334	323	176–407	endo, endo	55.13
OHPMPDA-Cd	II	489	484	407–648	endo	25.31
	Residue			>648		2.29

complex. OHPMPDA-Cr and OHPMPDA-Co have one decomposition step in the temperature ranges of 221–407°C and 222–731°C, respectively, corresponding to the decomposition of complexes. DTA profiles of these complexes present one endothermic peak at 210 and 212°C, respectively. These peaks are attributed to the melting of the complexes. Furthermore, TG analysis indicated that the initial decomposition temperature of OHPMPDA is higher than that of HPMPD. This can be attributed to the long conjugated band systems of OHPMPDA

According to TG analyses, mass losses of OHPMPDA-metal complexes changed at 1000°C as follows: OHPMPDA-Cu > OHPMPDA-Co > OHPMPDA > OHPMPDA-Ni > OHPMPDA-Mn > OHPMPDA-Fe > OHPMPDA-Cr > HPMPDA > OHPMPDA-Zn > OHPMPDA-Pb > OHPMPDA-Hg > OHPMPDA-Cd.

To check the thermal stabilities of the complexes in solid state, the initial decomposition temperatures of the complexes were compared. It was found that the thermal stabilities of HPMPDA, OHPMPDA, and OHPMPDA-metal complex compounds follow the following order: OHPMPDA > OHPMPDA-Co > OHPMPDA-Cr > HPMPDA > OHPMPDA-Cd > OHPMPDA-Zn > OHPMPDA-Pb > OHPMPDA-Hg > OHPMPDA-Fe > OHPMPDA-Mn > OHPMPDA-Cu > OHPMPDA-Ni.

It was found by Arshad et al. that the thermal stabilities of 1,2-dipiperidinoethane complexes of cobalt, nickel, zinc, and cadmium show an increase in the following sequence: Ni(II) < Co(II) < Cu(II) < Zn(II) < Cd(II).²⁴ On the other hand, in our previous study, the thermal stabilities of metal complexes of the oligo-2-[(4-morpholin-4-yl-phenyl)imino]methylphenol were found as Cu(II) > Co(II) > Zn(II) >

TABLE III
Kinetic Parameters of Thermal Decomposition Process of the Entire Compound

Materials	Stage	Methods	<i>n</i>	<i>E</i> (kJ mol ⁻¹)	ln <i>A</i> (s ⁻¹)	Δ <i>S</i> [#] (kJ mol ⁻¹)	Δ <i>H</i> [#] (kJ mol ⁻¹)	Δ <i>G</i> [#] (kJ mol ⁻¹)	<i>r</i>
OHPMPDA	I	MT	1.6	158.9 ± 0.155	38.25	67.99	154.3	116.7	0.99324
		vK	1.7	156.0 ± 0.242	46.09	133.2	151.4	77.62	0.98534
		MKN	1.6	148.8 ± 0.358	29.57	-4.207	144.2	146.5	0.98130
		WHYC	1.6	148.8 ± 0.372	29.45	-4.839	144.2	146.9	0.98123
		CR	1.6	148.5 ± 0.365	29.46	-5.095	143.9	146.7	0.98050
HPMPDA	I	HM	1.7	153.7 ± 0.251	11.37	-155.5	148.5	234.7	0.97824
		MT	1.2	78.72 ± 0.092	19.47	-89.35	73.41	130.4	0.99717
		Vk	1.3	81.58 ± 0.054	20.43	-81.34	76.27	128.1	0.99698
		MKN	1.2	68.59 ± 0.197	10.69	-162.3	63.28	166.8	0.99684
		WHYC	1.2	68.57 ± 0.197	10.61	-163.0	63.26	167.2	0.99683
OHPMPDA-Zn	I	CR	1.2	68.14 ± 0.196	10.48	-164.1	62.83	167.5	0.99680
		HM	1.2	82.58 ± 0.074	11.38	-156.5	77.27	177.1	0.97286
		HM	1.2	25.51 ± 0.089	9.911	-168.8	20.20	127.9	0.98707
		vK	1.0	22.64 ± 0.221	4.993	-209.7	17.33	151.1	0.98475
		MT	0.8	22.59 ± 0.179	8.553	-180.1	17.28	132.2	0.94827
OHPMPDA-Pb	I	WHYC	1.0	27.22 ± 0.644	0.054	-250.8	21.91	181.9	0.91714
		MKN	1.0	27.23 ± 0.644	0.045	-250.8	21.92	181.9	0.91714
		CR	1.0	16.62 ± 0.518	-0.681	-256.9	11.29	175.2	0.86359
		MT	1.0	126.2 ± 0.538	18.86	-98.12	117.8	216.0	0.98301
		WHYC	1.0	125.2 ± 0.124	9.055	-179.7	116.9	296.6	0.98303
	II	MKN	1.0	125.3 ± 0.124	9.089	-179.4	117.0	296.4	0.97303
		VK	1.2	122.7 ± 0.100	16.29	-119.5	114.3	233.9	0.94208
		CR	1.2	119.5 ± 0.132	10.24	-169.8	111.2	281.0	0.92146
		HM	1.2	123.8 ± 0.192	10.65	-166.3	115.5	281.9	0.90113
		vK	1.0	33.08 ± 0.365	9.080	-172.8	29.33	107.3	0.98732
OHPMPDA-Ni	I	HM	0.9	35.07 ± 0.058	10.30	-162.6	31.32	104.6	0.98589
		MT	0.8	34.17 ± 0.262	13.60	-135.2	30.42	91.40	0.98590
		WHYC	1.0	35.06 ± 0.629	5.556	-202.1	31.31	122.4	0.98573
		MKN	1.0	35.07 ± 0.629	5.568	-202.0	31.32	122.4	0.98573
		CR	1.0	30.41 ± 0.680	5.978	-198.6	26.66	116.2	0.97805
	II	vK	1.2	38.31 ± 0.119	12.18	-147.0	34.56	100.8	0.99639
		HM	1.3	36.99 ± 0.220	9.825	-166.6	33.24	108.4	0.99538
		MT	1.4	38.84 ± 0.087	10.15	-163.9	35.09	109.0	0.99266
		WHYC	1.2	36.85 ± 0.316	2.328	-229.0	33.10	136.3	0.99442
		MKN	1.2	36.87 ± 0.316	2.330	-229.0	33.12	136.4	0.99442
OHPMPDA-Mn	I	CR	1.3	36.48 ± 0.316	4.221	-213.2	32.73	128.9	0.99173
		MT	1.0	40.63 ± 0.228	17.72	-99.13	37.63	73.32	0.99411
		WHYC	1.0	40.63 ± 0.527	9.739	-165.5	37.63	97.22	0.99411
		MKN	1.0	40.63 ± 0.527	9.760	-165.3	37.63	97.16	0.99411
		vK	1.2	40.63 ± 0.361	17.44	-101.4	37.63	74.15	0.99338
	II	CR	1.1	40.63 ± 0.566	11.15	-153.7	37.63	92.98	0.99272
		HM	1.1	40.10 ± 0.062	10.19	-161.7	37.10	95.34	0.98876
		HM	0.3	27.02 ± 0.022	9.807	-169.3	21.71	129.7	0.99690
		vK	0.4	20.09 ± 0.057	1.923	-234.8	14.78	164.6	0.99198
		MT	0.4	21.54 ± 0.147	8.709	-178.4	16.23	130.0	0.98174
	III	MKN	0.8	25.49 ± 0.572	0.831	-243.9	20.18	175.8	0.96422
		WHYC	0.8	24.05 ± 0.573	1443	-130.8	18.74	102.2	0.93207
		CR	0.8	24.21 ± 0.522	0.116	-249.9	18.90	178.3	0.93467
		MT	2.3	174.7 ± 0.542	33.80	28.53	168.5	147.1	0.99324
		vK	2.3	172.8 ± 1.931	33.53	26.22	166.6	147.0	0.99202
OHPMPDA-Mn	I	MKN	2.5	173.2 ± 1.308	26.58	-31.56	167.0	190.5	0.99260
		WHYC	2.5	173.2 ± 1.308	26.50	-32.18	167.0	191.0	0.99260
		CR	2.5	172.8 ± 1.308	26.46	-32.53	166.6	190.9	0.99254
		HM	2.5	183.8 ± 0.081	12.67	-147.1	177.6	287.6	0.99022
		MT	2.4	38.41 ± 0.095	18.28	-93.62	35.69	66.22	0.99908
	II	HM	2.5	32.38 ± 0.080	9.742	-164.6	29.58	83.27	0.99361
		vK	2.5	33.32 ± 1.897	13.44	-133.9	30.60	74.27	0.99800
		MKN	2.5	33.91 ± 0.223	10.77	-156.1	31.19	82.09	0.99879
		WHYC	2.5	33.89 ± 0.223	10.70	-156.7	31.17	82.26	0.99879
		CR	2.5	33.64 ± 0.222	10.54	-158.0	30.92	82.44	0.99877
II	MT	1.4	73.54 ± 0.369	20.21	-82.21	68.80	115.5	0.98740	
	vK	1.4	71.49 ± 1.050	17.30	-1064	66.75	127.3	0.98215	

TABLE III. Continued

Materials	Stage	Methods	<i>n</i>	<i>E</i> (kJ mol ⁻¹)	ln <i>A</i> (s ⁻¹)	Δ <i>S</i> [#] (kJ mol ⁻¹)	Δ <i>H</i> [#] (kJ mol ⁻¹)	Δ <i>G</i> [#] (kJ mol ⁻¹)	<i>r</i>
OHPMPDA-Hg	III	MKN	1.4	72.59 ± 1.079	13.64	-136.8	67.85	145.7	0.98189
		WHYC	1.4	69.78 ± 0.980	12.95	-142.6	65.04	146.2	0.97949
		CR	1.5	72.22 ± 1.079	13.45	-138.4	67.46	146.2	0.96657
		HM	1.3	74.57 ± 0.152	11.07	-158.2	69.83	159.8	0.96657
		HM	0.2	65.13 ± 0.033	11.01	-162.6	57.50	206.6	0.99170
		vK	0.4	59.83 ± 0.224	7.281	-193.7	52.20	229.8	0.98189
		MT	0.4	59.34 ± 0.234	12.54	-150.0	51.71	189.2	0.97349
	IV	MKN	0.7	55.51 ± 0.888	4.609	-215.9	47.87	245.9	0.92513
		WHYC	0.7	55.48 ± 0.888	4.528	-216.6	47.85	246.5	0.92498
		CR	0.7	54.83 ± 0.886	4.336	-218.2	47.20	247.3	0.92343
		MT	1.9	351.4 ± 0.552	47.37	138.7	342.9	200.9	0.99429
		vK	2.0	355.3 ± 1.812	51.17	170.3	346.8	172.4	0.99410
		HM	1.9	352.9 ± 0.049	13.16	145.7	344.4	493.7	0.99264
		MKN	2.1	357.6 ± 1.329	39.92	76.77	349.1	270.5	0.99413
	I	WYHC	2.1	357.7 ± 1.329	39.84	76.08	349.2	271.3	0.99413
		CR	2.1	357.3 ± 1.329	39.84	76.08	348.8	270.9	0.99410
		CR	1.0	44.31 ± 0.158	10.72	-158.6	40.80	107.7	0.99746
		MKN	1.0	43.16 ± 0.186	12.88	-140.7	39.65	99.04	0.99733
		WHYC	1.0	42.24 ± 0.154	10.10	-163.8	38.73	107.8	0.99726
		MT	1.0	45.01 ± 0.282	5.205	-204.5	41.50	127.8	0.96815
		HM	0.8	45.19 ± 0.050	10.10	-163.8	41.68	110.8	0.96619
	II	vK	1.2	45.19 ± 0.050	10.10	-163.8	41.68	110.8	0.96619
		MT	0.4	88.9 ± 0.269	24.19	-48.76	84.36	110.9	0.99666
		vK	0.5	88.73 ± 0.462	22.46	-63.20	84.16	118.6	0.99630
		HM	0.4	89.32 ± 0.029	10.96	-158.7	84.78	171.4	0.99486
		MKN	0.7	88.69 ± 0.780	17.85	-101.5	84.15	139.5	0.99479
		WYHC	0.7	88.68 ± 0.780	17.77	-102.1	84.14	139.9	0.99478
		CR	0.7	88.35 ± 0.782	17.77	-102.1	83.81	139.5	0.99473
	III	MT	1.3	142.4 ± 0.897	32.08	15.89	137.3	127.5	0.94332
		vK	1.3	142.3 ± 0.481	37.71	62.66	137.2	98.93	0.93639
		Hm	1.4	144.4 ± 0.128	11.64	-154.8	139.3	233.6	0.93548
		MKN	1.4	139.9 ± 1.219	24.96	-43.30	134.8	161.3	0.93543
		WHYC	1.4	138.9 ± 1.192	24.89	-43.94	133.9	160.7	0.93497
		CR	1.4	139.6 ± 2.192	24.84	-44.33	134.5	161.7	0.93497
		MT	0.7	74.28 ± 0.097	13.29	-144.9	65.42	219.8	0.99353
	IV	WHYC	1.0	80.01 ± 0.278	4.646	-216.9	71.15	302.1	0.99160
		MKN	1.0	80.04 ± 0.278	4.667	-216.7	71.18	302.0	0.99160
		vK	1.0	82.73 ± 0.086	8.965	-180.9	73.87	266.6	0.99144
		CR	0.7	77.16 ± 0.538	6.187	-204.0	68.30	285.6	0.96735
		MC	0.7	74.28 ± 0.097	13.29	-144.9	65.42	219.8	0.99353
		MT	0.7	102.2 ± 0.888	39.65	83.82	99.48	71.40	0.98454
		Vk	0.8	104.4 ± 1.134	49.20	163.1	101.6	47.02	0.98311
I	MKN	0.7	102.2 ± 1.222	34.04	37.18	99.21	86.75	0.98203	
	WHYC	0.8	102.0 ± 1.222	33.97	36.59	99.23	86.97	0.98202	
	CR	0.8	101.8 ± 1.222	33.95	36.44	99.09	86.88	0.98191	
	Hm	0.8	101.0 ± 0.058	11.02	-154.4	98.29	149.9	0.98207	
	MT	1.4	122.9 ± 1.421	42.35	105.6	1199	81.78	0.98591	
	HM	1.5	122.2 ± 0.153	11.19	-153.6	119.1	174.6	0.97598	
	vK	1.5	124.7 ± 1.195	62.09	269.8	121.7	24.34	0.97596	
II	MKN	1.5	127.1 ± 1.568	38.15	70.69	124.1	98.59	0.95560	
	WHYC	1.5	127.1 ± 1.568	38.07	70.09	124.1	98.84	0.95558	
	CR	1.5	127.7 ± 1.568	38.07	70.05	123.9	98.70	0.95537	
	MT	1.1	35.63 ± 0.378	12.69	-144.2	31.10	109.6	0.98514	
	vK	1.2	36.09 ± 0.927	10.36	-163.7	31.56	120.6	0.98489	
	MT	0.8	34.22 ± 0.077	10.48	-162.8	29.69	118.2	0.97399	
	WHYC	1.0	33.25 ± 0.713	3.406	-221.6	28.72	149.2	0.96208	
III	MKN	1.0	33.26 ± 0.713	3.411	-221.5	28.77	149.2	0.96208	
	CR	1.0	31.92 ± 1.252	4.910	-209.1	27.39	141.1	0.88768	
	MT	1.3	181.8 ± 0.861	32.40	16.68	175.4	162.7	0.98497	
	Vk	1.4	181.1 ± 1.465	40.72	85.86	174.8	109.4	0.98459	
	MKN	1.3	181.2 ± 1.166	25.08	-44.11	174.8	208.5	0.98414	
	WYHC	1.3	181.2 ± 1.166	25.00	-44.82	174.8	209.0	0.97414	
	HM	1.1	180.3 ± 0.114	11.73	-155.0	173.9	292.2	0.94245	
IV	MT	1.3	181.8 ± 0.861	32.40	16.68	175.4	162.7	0.98497	
	Vk	1.4	181.1 ± 1.465	40.72	85.86	174.8	109.4	0.98459	
	MKN	1.3	181.2 ± 1.166	25.08	-44.11	174.8	208.5	0.98414	
	WYHC	1.3	181.2 ± 1.166	25.00	-44.82	174.8	209.0	0.97414	
	HM	1.1	180.3 ± 0.114	11.73	-155.0	173.9	292.2	0.94245	

TABLE III. Continued

Materials	Stage	Methods	<i>n</i>	<i>E</i> (kJ mol ⁻¹)	ln <i>A</i> (s ⁻¹)	Δ <i>S</i> [#] (kJ mol ⁻¹)	Δ <i>H</i> [#] (kJ mol ⁻¹)	Δ <i>G</i> [#] (kJ mol ⁻¹)	<i>r</i>
OHPMPDA-Cu	V	CR	1.3	180.7 ± 1.166	24.96	-45.16	174.4	208.8	0.94100
		MT	1.0	326.9 ± 2.234	47.04	136.9	319.3	194.5	0.98282
		WHYC	1.0	324.5 ± 2.145	36.77	51.57	316.9	269.9	0.98282
		MKN	1.0	324.6 ± 2.146	36.84	52.18	3171	269.5	0.97282
		CR	1.0	309.5 ± 2.154	36.73	51.26	302.0	255.3	0.96214
		Vk	1.0	309.7 ± 1.154	54.73	200.9	302.1	119.1	0.92283
	I	HM	1.0	309.2 ± 0.199	11.77	-156.3	301.6	444.0	0.91704
		MT	1.1	51.62 ± 1.305	22.15	-61.29	48.95	68.44	0.98286
		WHYC	1.0	49.03 ± 1.893	13.59	-132.4	46.38	88.50	0.98283
		MKN	1.0	49.05 ± 1.893	13.62	-132.2	46.40	88.44	0.98283
		vK	1.1	47.93 ± 1.945	20.97	-71.10	45.28	67.89	0.98192
		CR	1.1	48.11 ± 1.211	15.12	-119.7	45.46	83.54	0.95107
		HMm	1.2	47.33 ± 0.397	9.254	-168.5	44.68	98.27	0.95108
		II	MT	1.1	31.95 ± 0.093	10.30	-164.8	27.01	123.9
WHYC			1.0	30.21 ± 0.213	0.617	-245.4	25.32	169.6	0.98095
MKN			1.0	30.22 ± 0.213	0.611	-245.5	25.33	169.6	0.98095
VK	1.3		27.32 ± 1.890	4.603	-212.3	22.43	147.2	0.97276	
OHPMPDA-Cr	I	HM	1.3	28.24 ± 0.088	9.471	-171.8	23.35	124.3	0.96079
		CR	1.3	27.48 ± 0.316	2.054	-233.5	22.59	159.9	0.95138
		vK	1.0	87.29 ± 1.081	20.37	-81.42	82.23	131.7	0.99736
		HM	0.7	89.41 ± 0.093	11.98	-151.2	84.35	176.3	0.98642
		MT	1.0	84.37 ± 0.460	21.49	-72.15	79.31	123.1	0.98637
		WHYC	1.0	83.75 ± 1.061	12.87	-143.8	78.69	1661	0.96373
	I	MKN	1.0	83.79 ± 1.061	12.90	-143.5	78.73	166.0	0.96373
		CR	1.0	81.18 ± 1.193	14.17	-132.9	76.12	156.9	0.95201
		MT	1.1	26.67 ± 0.189	9.384	-175.2	19.94	161.7	0.99707
		WHYC	1.0	25.09 ± 0.418	-0.517	-257.5	18.36	226.7	0.98701
		MKN	1.0	25.11 ± 0.418	-0.530	-257.6	18.37	226.8	0.98701
		vK	1.1	24.25 ± 0.201	2.939	-228.8	17.52	202.6	0.96410
		HM	0.7	27.49 ± 0.151	10.44	-166.3	20.76	155.3	0.92401
		CR	1.3	22.14 ± 0.497	-0.143	-254.4	15.41	221.2	0.92454
OHPMPDA-Cd	I	vK	1.0	54.46 ± 0.513	12.35	-148.0	49.49	137.8	0.98692
		HM	0.7	55.47 ± 0.067	10.78	-161.0	50.50	146.6	0.98624
		MT	1.0	55.12 ± 0.334	15.79	-119.4	50.13	121.4	0.98618
		WHYC	1.0	54.73 ± 0.770	7.131	-191.4	49.73	164.0	0.98618
		MKN	1.0	54.72 ± 0.770	7.153	-191.2	49.75	163.9	0.96188
		CR	1.2	52.68 ± 0.942	8.527	-179.8	47.71	155.0	0.94047
	II	MT	1.2	91.44 ± 0.295	18.66	-97.45	85.14	158.9	0.99284
		WHYC	1.4	91.75 ± 0.525	18.10	-102.1	84.70	162.0	0.99131
		MKN	1.4	92.12 ± 0.077	11.07	-160.6	85.82	207.4	0.98799
		vK	1.4	89.19 ± 0.686	11.16	-159.8	82.89	203.9	0.98037
		CR	1.4	88.63 ± 0.686	11.03	-160.9	82.33	204.1	0.98022
		HM	1.4	92.12 ± 0.077	11.07	-160.6	85.82	207.4	0.97799

Zr(IV) > Pb(II) > Cd(II).²⁵ Consequently, we can assume that the coordination of metal ion to ligand is mainly responsible for thermal stabilities of the metal complexes.

Kinetic and thermodynamic study

To evaluate the decomposition processes and kinetic parameters of the presented compounds, TGA experiments were performed. The CR, HM, vK, MKN, MT, and WHYC methods were selected for kinetic analysis.

These methods are based on a single heating rate. Reaction order *n*, activation energy *E*, entropies Δ*S*[#], enthalpy change Δ*H*[#], free energy change Δ*G*[#], pre-exponential factor *A*, and linearization curves for

thermal decomposition of all materials have been elucidated from the TG curves using the methods mentioned above. From the TG/DTG and DTA curves, the activation energy, *E*, of the decomposition has been elucidated by the first one of the methods mentioned above, which has higher linear regression coefficient obtained for Arrhenius plots. The values of activation energy for the first decomposition stages of OHPMPDA, OHPMPDA-Fe, OHPMPDA-Cr, and HPMPDA were found to be 158.9 kJ mol⁻¹ according to MT, 102,21 kJ mol⁻¹ according to HM, 87,29 kJ mol⁻¹ according to vK, and 78.72 kJ mol⁻¹ according to MT. In this way, other compounds were in the range about from 22 to 49 kJ mol⁻¹. The results obtained and MT plots of

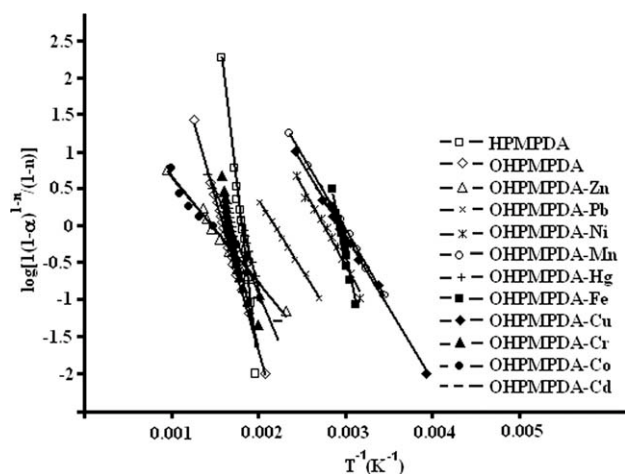


Figure 3 MT plots of first decomposition stage of HPMPDA, OHPMPDA and all OHPMPDA-metal complexes.

first decomposition stage of HPMPDA, OHPMPDA, and all OHPMPDA-metal complexes are given in Table III and Figure 3.

For all the methods, determination of preexponential factor and reaction order is possible from the expression of $g(\alpha)$ in eq. (3) and $n \neq 1$:

$$g(\alpha) = \frac{1 - (1 - \alpha)^{1-n}}{1 - n}$$

The results are in harmony with the values obtained for all of them. The results indicate that the values of all methods are comparable. As seen in Table III, the values of correlation coefficients for the linearization curves of HPMPDA, OHPMPDA, and OHPMPDA-metal complexes are ~ 1.00 , and the values of reaction orders are around 1.00 for complex compounds. The kinetic data obtained by different methods are in good agreement with each other. The enthalpy change ΔH^\ddagger , entropy change ΔS^\ddagger , and the Gibbs free energy change ΔG^\ddagger of all the complexes were calculated using eqs. (9), (10), and (11), respectively. The thermodynamic parameters

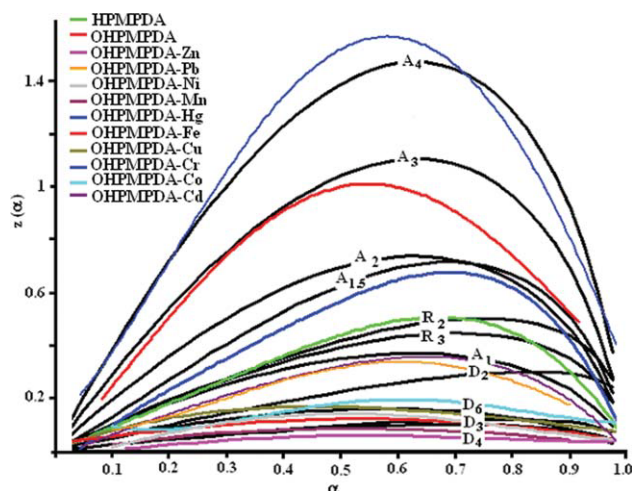


Figure 4 Master curves of $z(\alpha)$ and experimental data. [Color figure can be viewed in the online issue, which is available at www.interscience.wiley.com.]

calculated are reported in Table III. According to DTG curves, several complexes have negative entropies. This result indicates that the studied complexes exhibit more ordered systems than reactants.²⁶

On the other hand, theoretical master curves are often used as a reference to find out the reaction mechanism for the studied systems. According to Criado et al., a master plot is a characteristic curve independent of the condition of the measurement. The master curve plots of $z(\alpha)$ versus α for different mechanisms have been illustrated in Figure 4. The mechanism functions related to the thermal decomposition processes are given in Table IV.

The experimental data of $z(\alpha)$ for OHPMPDA and OHPMPDA-metal complexes agree very well with D_n , which corresponds to a deceleration mechanism and A_n master curve. Although the decompositions of OHPMPDA are of D_n type, OHPMPDA-metal complexes have generally A_n mechanisms.

The activation energy E and Gibbs free energy change ΔG^\ddagger (Figs. 5 and 6) change with the increase of atomic number in the third series of d-block

TABLE IV
Kinetic Functions in Relation to HPMPDA, OHPMPDA and OHPMPDA-metal Complexes

Compound	I Step	II Step	III Step	IV Step	V Step
HPMPDA	R ₂				
OHPMPDA	D ₆				
OHPMPDA-Zn	D ₄	D ₆			
OHPMPDA-Pb	A ₁	D ₂			
OHPMPDA-Ni	D ₆	A ₂	A ₃		
OHPMPDA-Mn	D ₄	A ₃	A ₄	A ₃	
OHPMPDA-Hg	A ₄	A ₃	A ₃	A _{1.5}	
OHPMPDA-Fe	A ₃	A ₄	D ₆	A ₄	A _{1.5}
OHPMPDA-Cu	D ₆	A ₄			
OHPMPDA-Cr	A _{1.5}				
OHPMPDA-Co	D ₆				
OHPMPDA-Cd	A ₁	D ₁			

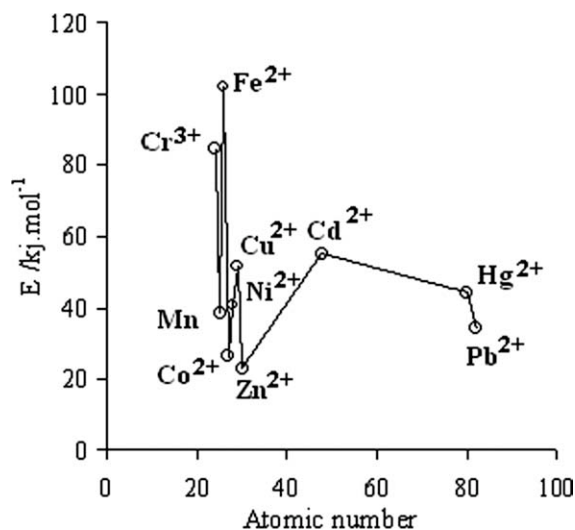


Figure 5 Activation energy E of divalent metal ions of complexes vs atomic number: the first decomposition stage.

elements for OHPMPDA–metal complexes. The complexes of Cr^{3+} , Fe^{2+} , Cu^{2+} , and Cd^{2+} with OHPMPDA are present on the peaks of the energy curve. This means that these complexes are more stable at the beginning of decomposition than those on the bottom of the curve (Mn^{2+} , Co^{2+} , Ni^{2+} , Zn^{2+} , Hg^{2+} , and Pb^{2+} complexes).

CONCLUSIONS

A study on the thermal decomposition of HPMPDA, OHPMPDA, and OHPMPDA–metal complexes was carried out with several kinetic methods. The thermal decomposition kinetic was investigated through the evaluation of the dynamic TG data obtained at a single heating rate. Thermal data obtained were

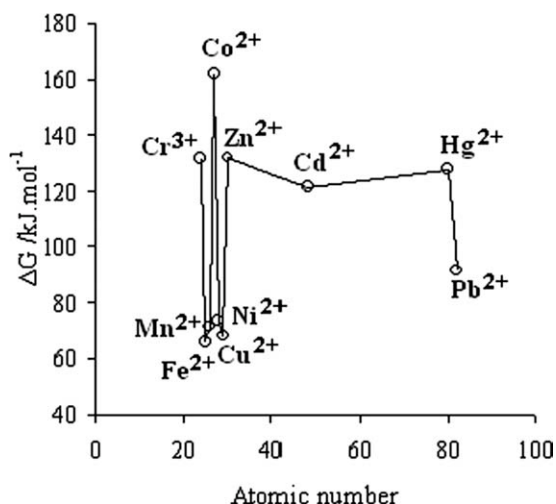


Figure 6 Gibbs free energy change ΔG^* of divalent metal ions of complexes vs atomic number: the first decomposition stage.

evaluated with CR, HM, vK, MKN, MT, and WHYC methods and with the Criado-Malek-Ortega method for kinetic analysis. The activation energy values obtained with CR, HM, vK, MKN, MT, and WHYC methods were in good agreement with one another. The experimental results suggested that the actual decomposition mechanisms of HPMPDA, OHPMPDA, and OHPMPDA–metal complex compounds were generally a decelerated D_n and sigmoidal A_n types. It was found that the thermal stabilities of the HPMPDA, OHPMPDA, and OHPMPDA–metal complex compounds for the first decomposition stage followed the orders: OHPMPDA > OHPMPDA-Co > OHPMPDA-Cr > HPMPDA > OHPMPDA-Cd > OHPMPDA-Zn > OHPMPDA-Pb > OHPMPDA-Hg > OHPMPDA-Fe > OHPMPDA-Mn > OHPMPDA-Cu > OHPMPDA-Ni.

References

1. Arimoto, F. S.; Haven, A. C., Jr. *J Am Chem Soc* 1955, 77, 6295.
2. Karabulut, S.; Aydođdu, C.; Düz, B.; İmamođlu, Y. *J Inorg Organomet Polym Mater* 2006, 16, 115.
3. Antony, R.; Tembe, G. L.; Ravindranathan, M.; Ram, R. N. *Polymer* 1998, 18, 4327.
4. Chantarassiri, N.; Tuntulani, T.; Tongroung, P.; Seangprasertkit, R.; Wannarong, W. *Eur Polym J* 2000, 36, 695.
5. Maurya, M. R.; Kumar, A.; Manikandan, P.; Chand, S. *Appl Catal A* 2004, 277, 45.
6. Kaya, I.; Bilici, A. *J Macromol Sci Pure Appl Chem* 2006, 43, 719.
7. Kaya, I.; Bilici, A. *J Appl Polym Sci* 2006, 102, 3795.
8. Kaya, I.; Bilici, A. *J Appl Polym Sci* 2007, 105, 1356.
9. Mart, H.; Vilayetođlu, A. R. *Polym Degrad Stab* 2004, 83, 255.
10. Cazacu, M.; Marcu, M.; Vlad, A.; Rusu, G. I.; Avadane, M. *J Organomet Chem* 2004, 689, 3005.
11. Tuncel, M.; Özbülbül, A.; Serin, S. *React Funct Polym* 2008, 68, 292.
12. Oriol, L.; Alonso, P. J.; Martinez, J. I.; Pídol, M.; Serrano, J. L. *Macromolecules* 1994, 27, 1869.
13. Coats, A. W.; Redfern, J. P. *Nature* 1964, 201, 68.
14. Horowitz, H. H.; Metzger, G. *Anal Chem* 1963, 35, 1464.
15. Madhusudanan, P. M.; Krishnan, K.; Ninan, K. N. *Thermochim Acta* 1993, 221, 13.
16. Van Krevelen, D. W.; Herden, C.; Huntjens, F. J. *Fuel* 1951, 30, 253.
17. Wanjun, T.; Yuwen, L.; Hen, Z.; Cunxin, W. *Thermochim Acta* 1993, 408, 39.
18. MacCallum, J. R.; Tanner, J. *Eur Polym J* 1970, 6, 1033.
19. Criado, J.; Malek, J.; Ortega, A. *Thermochim Acta* 1989, 147, 377.
20. Kaya, I.; Bilici, A.; Saçak, M. *Synth Met* 2009, 159, 1414.
21. Senum, G. I.; Yang, K. T. *J Therm Anal Calorim* 1977, 11, 445.
22. Al-Wallan, A. A. *Synth React Inorg Met-Org Chem* 2002, 32, 489.
23. Dođan, F. Ph.D. Thesis, Ege University, Izmir, Turkey, 2006.
24. Arshad, M.; Rehman, S.; Khan, A. S.; Masud, K.; Arshad, N.; Ghani, A. *Thermochim Acta* 2002, 364, 143.
25. Dođan, F.; Kaya, I. *Des Monom Polym* 2007, 10, 527.
26. Sekerci, M.; Yakuphanoglu, F. *J Therm Anal Calorim* 2004, 75, 2004.